THE IMPACT OF A WIDEBAND CHANNEL ON UWB SYSTEM DESIGN

Mike S.W. Chen and Robert W. Brodersen
Berkeley Wireless Research Center
Berkeley, CA

ABSTRACT

The goal of this work is to investigate the unique system implementation issues associated with an ultra-wideband channel. The paper begins with channel models and from the characteristics of these models, the cost of doing coherent detection, including channel estimation and maximum ratio combining, is analyzed and simulated. The results show that using a signal bandwidth ranging over 500MHz to 2 GHz has better system performance than using the entire available 7 GHz bandwidth. It is also shown that matched filtering in UWB plays a more critical role than in a narrowband system. Finally, the impact of imperfect matched filtering is analyzed and simulated.

I. INTRODUCTION

Communication system design is strongly tied to the characteristics of the wireless channel. Without good knowledge of the channel model, it is difficult to come up with reliable system specifications and architectures. In narrowband systems, the signal bandwidth is much smaller than the carrier frequency. Therefore, central limit theorem can be applied to channel modeling, where Raleigh and Rician distributions are the most commonly used models [1][2]. However, as signal bandwidth scales up, assumptions that are made for narrowband system begin to break down. In section II, we briefly revisit important channel characteristics, such as frequency dependency and coherence time, and discuss their potential influence on UWB system design. Some statistical models reported in the literature are also summarized.

In section III, we apply these wideband channel models to a coherent receiver architecture, which can inherently take full advantage of a wideband signal. The performance of doing coherent detection, mainly channel estimation and maximum ratio combining, is analyzed. The analyzed receiver architecture makes use of a matched filter and Linear Least Square Estimator (LLSE) for lower system complexity, and performs hard decision at the end for BER analysis. Important system design parameters, such as optimal signal bandwidth and energy capturing period are explored through simulations and analytical equations. The work extends from the analytical approach in [3], where a simple uniform distributed channel model was assumed. Finally, due to the frequency dependency of the wireless channel as well as estimation error, a discrepancy between incoming signal waveform and matched filter response exists, and degrades the total system performance. For instance, the scattered waveform can vary due to different geometry and type of objects [4][5]. The impacts from these channel uncertainties are analyzed and simulated in section IV.

II. UWB CHANNEL MODELING

UWB is allowed to transmit between 3.1GHz to 10.6GHz for indoor communication systems [6]. The relationship between transmitted waveform, $\Phi(t)$, and received waveform, $y(t)$, can be expressed as a function of channel gain, $a_i(f,t)$ and arrival time $\tau_i(f,t)$ of ith multipath:

$$y(t) = \sum_{i=1}^{L} a_i(f,t)\phi(t-\tau_i(f,t)) \qquad (1)$$

Assuming the system is bandlimited to W, the above continuous time relationship can be represented as a discrete-time version using the sampling theorem [7].

$$y[m] = \sum_{k=-\infty}^{m} h[k,m]x[m-k]$$
$$h[k,m] = \sum_{i=1}^{L} a_i(f,m/W)e^{j2\pi f_c \tau_i(f,m/W)}\,\mathrm{sinc}(k-W\tau_i(f,m/W)) \qquad (2)$$

Next, some insights based on these equations are provided.

- Frequency dependency:

In narrowband system, the data bandwidth, W, is assumed much smaller than carrier frequency, f_c. Therefore, the analysis in narrowband system assumes channel gain and delay, $a_i(t)$ and $\tau_i(t)$, are frequency independent within the bandwidth of interest. This allows us to treat the received signal as the summations of delayed and scaled versions of transmitted signals, which is also known as the multipath model. Basically, the received signal shape does not change over wireless channel. The receiver can thus use an expected waveform as the matched filter response.

However, the UWB signal bandwidth is so wide that the frequency dependency on tap gain and delay cannot be ignored. In other words, the received signal waveform gets distorted by the communication channels, such as antenna pattern, propagation through frequency selective objects, circuit impairments, etc. This phenomenon inspires us to do a further analysis on this pulse shape uncertainty, which is addressed in the later section.

• Coherence time:

There are several reasons for the time variation of channel response. The first one is Doppler spread, which is the relative difference of Doppler shifts of every multipath contributing to a certain discrete channel tap. Doppler shift of the i[th] multipath can be expressed as $f_c\tau_i'$, and is essentially the phase rotation introduced by the carrier sinusoid as shown in Eq. (2). Since a pulse-based UWB radio performs carrierless communication, there is no Doppler shift associated with the carrier.

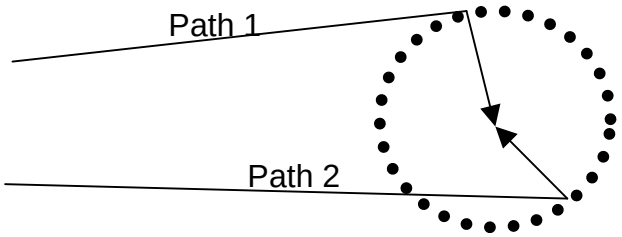

Figure 1. Multipaths arrive from all directions

Shown in Figure 1, we assume all the multipaths uniformly come from all directions. The channel response of one particular tap is the summation of all the multipaths that propagate about the same distance, *d*. Assuming the mobile moves at speed, *v*, the channel response can be expressed as,

$$\sum A_i \cdot u(t - \frac{d}{c} - \frac{v}{c}\cos\theta_i \cdot t) \qquad (3)$$

As mentioned earlier, there is no phase construction or destruction for a carrierless UWB system. However, there is still Doppler effect on the pulse waveform, which is a frequency drift of $(1 - \frac{v}{c}\cos\theta_i)$. Given an indoor environment with 1 m/sec movement, frequency drift effect is negligible due to the small ratio to speed of light, c. Therefore, we conclude that a carrierless UWB system does not suffer from Doppler spread. Even for a carrier-based UWB, such as multi-band OFDM approach, there is still less Doppler spread compared to a narrowband system due to fewer multipaths contributing to one channel tap. The coherence time under 1m/sec scenario is on the order of 10's of milliseconds to second, which allows ample time for channel estimation.

Another important factor causing time variation is the movement of multipaths between discrete channel taps, which can be described as $W^* \tau_i'$, shown in Eq. (2). The bandwidth in narrowband systems is much smaller than the center frequency so that the movement of multipaths is negligible compared to Doppler spread. However, in UWB, the bandwidth is comparable to center frequency. Thus, the time scale of multipath movement is of the same order of magnitude as the Doppler shift, i.e. 10's of milliseconds to second in an indoor environment. The time variation of channel gain, $a_i(f, t)$, depends on the free space attenuation. Assuming receiver and transmitter move locally compared to the distance between the two, the channel gain varies slowly compared to the previous ones.

From simple calculations, the coherence time is comparable to that of narrowband systems with GHz center frequency. Note that the frequency dependence of the channel gain and delay can also be time varying. For example, if a frequency selective object moves within the channel, it will cause a time-varying pulse shape. In indoor environment, this effect should be negligible.

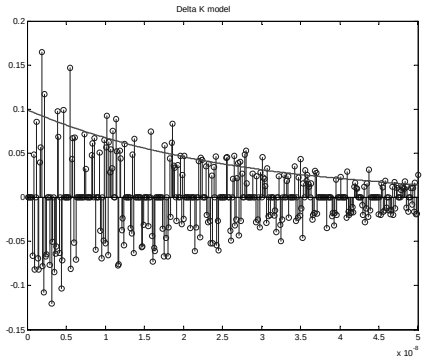

Figure 2 One Realization of Delta-K model

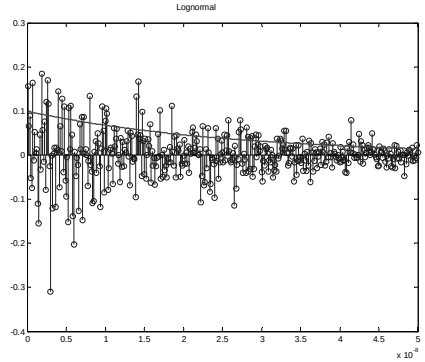

Figure 3 One Realization of Lognormal Model

• Statistical model:

Several statistical models are proposed in the IEEE 802.15 study group. Because UWB occupies a wider bandwidth, the number of multipaths contributing to one channel tap is less than in narrowband systems. Less averaging effects imply Rayleigh model is no longer suitable. Different parties have proposed individual model that fit their own measurement and are summarized as follows:

(1) Saleh-Valenzuela Model (S-V):

S-V model does not assume multipaths arrive on each sampling time. Two Poisson processes are used to describe the channel. The first one is for the first path of each path cluster and the second one is for the paths within each cluster. Tap magnitude is Rayleigh distributed [8].

(2) Δ-K model:

This is proposed in [9]. A path arrives within time duration Δ according to a certain probability. The tap magnitude is lognormal distributed. It simulates different environment by changing different parameters, as shown in [10].

(3) Nakagami model:

Nakagami distribution is usually used when the central limit theorem does not hold [11].

(4) Lognormal model:

Lognormal model assumes Rayleigh distribution with exponentially decaying power gain. This model is used to verify the analytical analysis given in this paper.

III. ANALYSIS AND SIMULATIONS OF COHERENT RECEIVER

In order to exploit the diversity gains from the large bandwidth in UWB, we need a coherent receiver, i.e. Rake combining, at the cost of more complexity. In the following sections, we will analyze the performance of coherent detection in order to determine optimal signal bandwidth, as well as the number of multipaths receiver should collect in the Rake combining scheme. The time period which receiver captures multipaths is referred as collection time in the following sections.

UWB has a maximum available bandwidth of 7.5 GHz. An important system specification is that how much bandwidth one should use for optimal performance. Although wider transmission bandwidth implies more diversity, the estimation error would increase if one fixed the total transmission power. On the other hand, if the transmission power increases in proportion with the bandwidth, then it is not surprising that the performance is always better by scaling up bandwidth, because the estimation error remains the same while diversity gain enhances the performance. From circuit implementation perspective, a low-power and low-cost UWB radio that adopts an integrated CMOS solution [12] is however limited by the maximum output voltage. As a consequence, the output power cannot be scaled up arbitrarily with the bandwidth. Given a power-constrained system implementation, we fixed the total transmission power for the following analysis.

A Linear Least Square Error (LLSE) estimator was used for channel estimation. Although LLSE estimator is not as optimal as MMSE, it does simplify the hardware implementation. Plus, it is a robust estimator for any stochastic process to be estimated. Therefore, we choose LLSE in this project, but may still explore the best estimator for UWB channel estimation in the future. For the maximum ratio combining scheme, LLSE estimation result is used as filter response, while a hard decision is made for error rate analysis.

• Channel estimation:

In the case of L resolvable paths, we express the received signal in vector form.

$$\vec{y} = \sum_{i=1}^{L} h[i]\vec{u} + \vec{w}$$

The received vector, $\vec{u}$, is assumed orthogonal over different resolvable path. As the bandwidth scales up, the number of resolvable paths should increase. Note that UWB pulse, bandlimited to *W*, has a certain shape and duration and may not meet the Nyquist criteria. Therefore, there could be an ISI problem between samples spaced by 1/*W*. The following analysis and simulation assumes the pulse energy is mostly confined within 1/*W* period or a clean algorithm is adopted to maintain orthogonality over different channel taps.

Before we perform LLSE estimation, the incoming signal is processed by a matched filter in order to project the signal information onto the correct dimension. In this section, we assume the receiver perfectly knows the incoming signal shape. In the next section, we will consider an imperfect matched filter, which causes extra estimation error.

By mapping received signal, $\vec{y}$, onto signal dimension, $\vec{u}$, we get sufficient statistics, $r^{(\ell)}(t)$, at path ℓ,

$$r^{(l)} = \frac{\vec{u}^{(l)}}{\|\vec{u}\|} \cdot \vec{y}$$

Next, extra processing gain is provided by averaging $r^{(l)}$ K times, and the estimated channel response and the estimation error for tap ℓ are derived:

$$\hat{h}_l = \frac{\sqrt{\varepsilon} \cdot E(h_l^{\,2})}{\varepsilon \cdot E(h_l^{\,2}) + \frac{No}{2K}} \cdot \left(\frac{1}{K}\sum_{1}^{K} r_k^{(l)}\right)$$

$$\sigma_e^{\,2} = \frac{E(h_l^{\,2}) \cdot \frac{No}{2K}}{\varepsilon \cdot E(h_l^{\,2}) + \frac{No}{2K}}$$

where ε is the signal energy; and No is the channel noise density.

- Rake combining:

The error event of the Rake combining using the estimated channel response is when the receiver detects "zero" while transmitter sends "one", and vice versa. The error probability can be expressed as,

$$Pe = P(V0 > V1) = P\left(\sum_{i=1}^{L} \hat{h}[\ell](W0 - W1 - h[\ell] \cdot \sqrt{\varepsilon}) > 0\right) = P(X > 0)$$

where *V1, V0* (*W1, W0*) is the detection energy (noise energy) with and without signal existence

The summation of polynomial functions of tap coefficients is not easy to compute. So, we treat the whole summation as a random variable X. By computing the first and second moment of X, one can gain some insights about the error probability function. The mean and variance of X is as follows,

$$E(X) = -\sum_{1}^{L} \frac{\sqrt{\varepsilon} \cdot E(h_l^{\,2})}{\varepsilon \cdot E(h_l^{\,2}) + \frac{No}{2K}} \cdot \varepsilon \cdot E(h_l^{\,2})$$

$$Var(X) = \sum_{l=1}^{L} \left(\frac{\sqrt{\varepsilon} \cdot E(h_l^{\,2})}{\varepsilon \cdot E(h_l^{\,2}) + \frac{No}{2K}}\right)^2 \cdot \left(E(h_l^{\,2}) \cdot \varepsilon \cdot \left(\frac{No(K+1)}{2K}\right) + \frac{No}{2}\frac{No}{2K}\right)$$

- Simulations:

The following simulation results are based on a received SNR of 10 dB. The number of extra averaging cycles, K, is 10. The high received SNR is assuming there is processing gain already provided in order to reduce the simulation time. The smaller the incoming SNR, the more processing gain one should provide to the channel estimator and Rake combiner. The channel models we used were Δ-K model and lognormal model. All the simulations were compared to previous error probability analysis assuming random variable X is Gaussian distributed. The channel we used in the simulation assumes a mean excess delay of 13 ns, and maximum collection time of 50 ns.

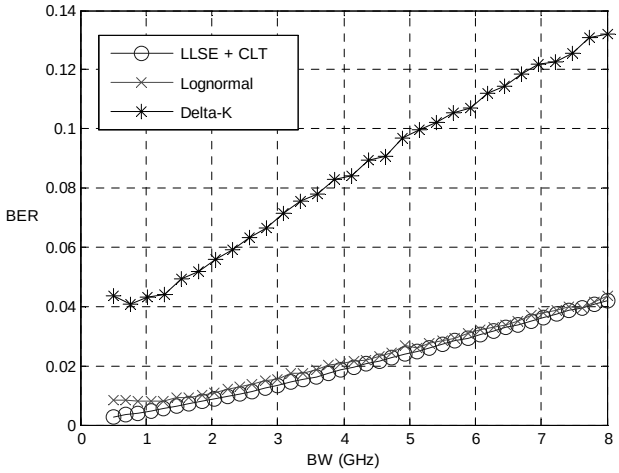

Figure 4. BER vs. Bandwidth

1) BER vs. bandwidth scaling

As we increased the bandwidth from 500 MHz to 8 GHz, the resolvable paths also increased from 25 to 400 paths given the delay spread of 50 ns. Since the total transmission power is currently fixed, the summation of all tap power is always constant. In other words, the more paths in the system the less energy resides in each path. Shown in Figure 4, the BER goes up with bandwidth after about 1GHz, where the estimation error overwhelms the diversity gain. Note that the analytical equations with CLT assumptions (X is Gaussian distribution) match closely with the simulation results for lognormal model. The performance of Δ-K model is much worse, because multipaths do not exist for every discrete tap. However, all channel models show that using bandwidth more than 2 GHz would increase the error rate.

2) BER vs. collection time

The above example is simulated by collecting all multipaths within 50 ns. Since the power delay profile is assumed to be exponentially decaying, there is no benefit to collecting more than needed. The signal collected in the tail results in more estimation error than signal energy. Therefore, we vary the collection time at different frequencies, shown in Figure 5 and 6. The performance does not improve much after collecting 10 ns for 8 GHz case, while 20 ns is sufficient for 500 MHz BW.

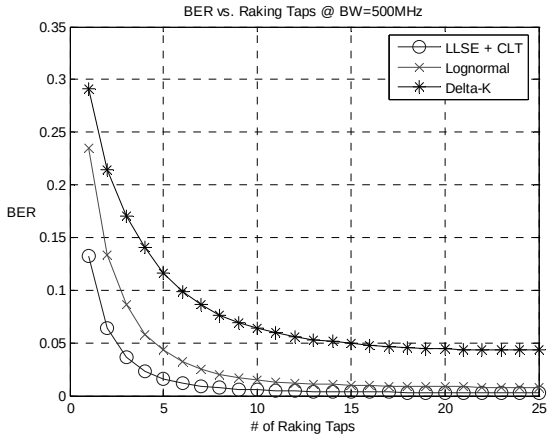

Figure 5 BER vs. Collection time for 500 MHz signal BW

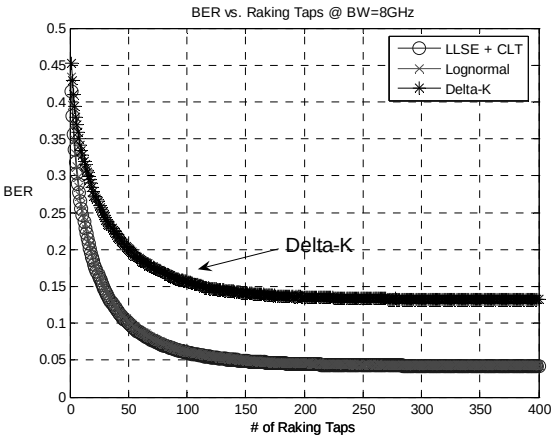

Figure 6 BER vs. Collection time for 8 GHz signal BW

IV. IMPACT OF DISTORTED MATCHED FILTER

As we described in the channel characteristics section, there is more significant distortion due to the wideband channel since the receiver cannot perfectly match to the incoming signal. In this section, we model the filter and analyze the performance degradation.

- Modeling matched filter:

The received signal, *y(t)*, is the combination of channel gain, *h*, and waveform distortion, *δ(t)*, plus white Gaussian noise, *n(t)*, caused by ambient, circuit or quantization noise.

$$y(t) = h \cdot (s(t) + \delta(t)) + n(t), \text{ where } n(t) \sim N(0, No/2)$$

Meanwhile, the matched filter response, *p(t)*, matches to the original expected waveform, *s(t)*, plus white Gaussian noise, *w(t)*, due to quantization error if a digital matched filter is adopted.

$$p(t) = s(t) + w(t) \qquad \text{,where } w(t) \sim N(0, Wo/2)$$

The output SNR of the matched filter is defined as the mean and variance ratio at the output of the filter. The following equation shows the relationship between output SNR with these nonidealities, δ(t) and w(t), and ideal SNR assuming a perfect matched filter.

$$SNR_{out} = \frac{(1+\frac{\int_0^T s(t)\delta(t)dt}{E_b})^2}{1+\frac{Wo}{No}+\frac{1}{SNR_{MF}}+\frac{\int_0^T \delta^2(t)dt}{E_b}+\frac{\int_0^T s(t)\delta(t)dt}{E_b}} SNR_{ideal}$$

The equation provides insights of how much SNR degradation would be caused by δ(t) and w(t).

- Imperfect matched filter impact on channel estimation:

We incorporate the matched filter nonideality, δ(t), into LLSE estimation as follows,

$$\vec{y} = \sum_{i=1}^{L} h[\ell] \cdot (\vec{u} + \vec{\delta}) + \vec{w}$$

$$r^{(l)} = \frac{\vec{u}^{(l)}}{\|\vec{u}\|} \cdot \vec{y} = h[\ell] \cdot \sqrt{\varepsilon} + (\vec{w}^{(l)} + \frac{\vec{u} \cdot \vec{\delta}}{\|\vec{u}\|} \cdot h[\ell])$$

Given the fact that signal energy always gets attenuated after channel propagation, we have the following inequality,

$$\|\vec{u} + \vec{\delta}\| < \|\vec{u}\| \Rightarrow \Delta < -\frac{\|\vec{\delta}\|^2}{2 \cdot \|\vec{u}\|} \qquad \text{,where } \Delta = \frac{\vec{u} \cdot \vec{\delta}}{\|\vec{u}\|}$$

The new estimation error has been added by an extra term due to distorted matched filter response:

$$\sigma_e^{\,2} = \sigma_{e,org}^{\,2} + \sigma_{e,extra}^{\,2} \qquad \text{,where}$$

$$\sigma_{e,extra}^{\,2} = \Delta \cdot E(h_l^{\,2}) \cdot \frac{\sqrt{\varepsilon} \cdot E(h_l^{\,2})}{\varepsilon \cdot E(h_l^{\,2}) + \frac{No}{2K}} \cdot (\frac{\sqrt{\varepsilon} \cdot E(h_l^{\,2})}{\varepsilon \cdot E(h_l^{\,2}) + \frac{No}{2K}} \cdot \Delta - 2)^2$$

We calculate the lower bound of the extra error. It is not intuitive from the above equation. Therefore, we plot the original (gray) and extra (black) estimation error at each channel tap and compared with two different averaging cycles of doing LLSE channel estimation, as shown in Figure 7 and 8.

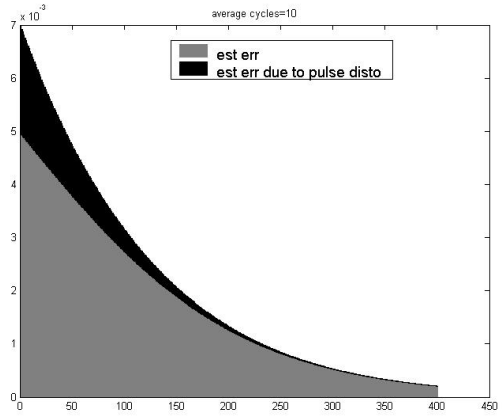

Figure 7 σ_{org} vs. σ_{extra} for 10 average cycles

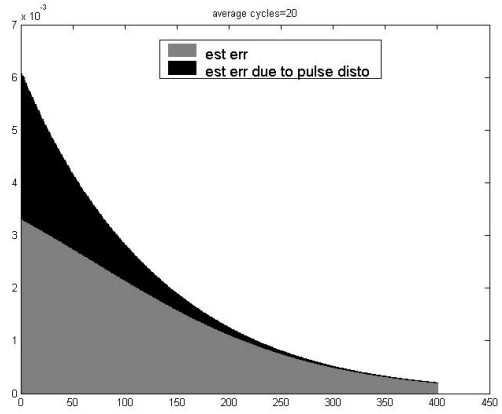

Figure 8 σ_{org} vs. σ_{extra} for 20 average cycles

From the above results, the extra estimation error due to distorted matched filter gradually dominates the estimation error as we try to get more accurate channel estimation by performing more averaging cycles. Intuitively thinking, this is because coherent detection is based on the outcomes of the matched filter. If there is any nonideality in the matched filter, more averaging will cause error accumulation, which in turn degrades system performance.

V. CONCLUSION

For a power-constrained system, it appears that using 500 MHz to 2 GHz signal bandwidth is adequate for coherent detection, and the optimal collection time should be a function of mean excess delay. There is no benefit to collecting all the multipaths, because the power delay profile is usually exponentially decaying. The impact of the matched filter nonideality has been analyzed and simulated. The results show that this nonideality is a potential difficulty of implementing a coherent UWB system.

VI. ACKNOWLEDGMENT

The authors would like to thank Prof. Tse (UC Berkeley) for valuable discussions. The project was supported by Army Research Office, North Carolina(Award No. 065861), and industrial members of the Berkeley Wireless Research Center.

VII. REFERENCES

[1] T. Rappaport, S. Seidel, and K. Takamizawa, " Statistical channel impulse response models for factory an open plan building radio communication system design," IEEE Trans. Commun., Vol. 39, May 1991, pp. 794-807.

[2] G. Turin, W. Jewell, and T. Johnston, " Simulation of urban vehicle-monitoring systems," IEEE Trans. Vehicular Tech., Vol. 21, No. 1, Feb. 1972, pp. 9-16.

[3] E. Telatar, and D. Tse, " Capacity and Mutual Information of Wideband Multipath Fading Channels," IEEE Trans. Info. Theory, Vol. 46, Jul. 2000, pp. 1384-1400.

[4] R. Qiu, " A Study of the Ultra-Wideband Wireless Propagation Channel and Optimum UWB Receiver Design," IEEE JSAC, Vol. 20, No. 9, Dec. 2002, pp. 1628-1637.

[5] Y. Zhang, M. Geyer, and E. Spitzer, " Time-Domain Waveform Development During Propagation and Scattering," Microwave and Optical Technology Letters, Vol. 26, No. 4, Aug. 2000, pp. 254-258.

[6] FCC, First Report and Order, FCC 02-48, Feb. 14, 2002.

[7] D. Tse, EE290S Class Notes, UC Berkeley, Fall 2002.

[8] A. Saleh and R. Valenzuela, " A Statistical Model for Indoor Multipath Propagatoin," IEEE JSAC, Vol. SAC-5, No. 2, Feb. 1987, pp. 128-137.

[9] H. Suzuki, "A Statistical Model for Urban Radio Propagation," IEEE Transactions on Communications, pp. 673-680, July 1977.

[10] H. Hashemi, "Impulse Response Modeling of Indoor Radio Propagation Channels," IEEE JSAC, Vol. 11, No. 7, Sept. 1993 pp. 967-978.

[11] A. Molisch, M. Win, and D. Cassioli, "The Ultra-Wide Bandwidth Indoor Channel: from Statistical Model to Simulations," IEEE P802.15-02/284-SG3a and IEEE P802.15-02/285-SG3a.

[12] I. O'Donnell, M. Chen, S. Wang and R. Brodersen, " An Integrated, Low Power, Ultra-wideband Transceiver Architecture for Low-rate, Indoor Wireless Systems," IEEE CAS, Workshop on Wireless Comm. and Networking, Sep. 2002.